

## **VIII- II -1. Project Research**

### **Project 2**

Y. Ohkubo

Research Reactor Institute, Kyoto University

### Objective and Participating Research Subjects

The main objectives of this project research are the investigation of the local properties of materials using short-lived radioactive nuclei and its related subjects.

This period is the final year of the project, in which period the reactor was restarted for use in joint research after an interval of 4 years.

The research subjects (PRS) executed in this period are as follows:

PRS-1 Newly Available Fission Products at KUR-ISOL (A. Taniguchi *et al.*).

PRS-2 Decay Spectroscopy of  $^{147}\text{La}$  with a Total Absorption Clover Detector (M. Shibata *et al.*).

PRS-3 Level Lifetime Measurements of Mass-Separated  $^{148}\text{Pr}$  (Y. Kojima *et al.*).

PRS-4 (a) Interaction of In and Cd Impurities in ZnO; (b) Observation of a Local Field at the  $^{111}\text{Cd}$  ( $\leftarrow^{111\text{m}}\text{Cd}$ ) Probe in Al-Doped ZnO (Y. Ohkubo *et al.*).

PRS-5 Mössbauer Study of  $\text{LaFeAsO}$  and  $\text{LaFeAsO}_{1-x}\text{F}_x$  in External Magnetic Fields (M. Seto *et al.*).

PRS-6 Dynamics of Mavicyanin Observed by the PAC Method Using  $^{111}\text{Cd}$  ( $\leftarrow^{111}\text{Ag}$ ) Probe (A. Yokoyama *et al.*).

PRS-7  $^{129}\text{I}$  Mössbauer Study of Superionic Silver Iodide Nanoparticles (R. Makiura *et al.*).

### Main Results and Contents of This Report

In order to extend the region in the nuclear chart of usable unstable nuclei at KUR-ISOL, A. Taniguchi *et al.* (PRS-1) searched for heavy Sr isotopes and have confirmed that  $^{97}\text{Sr}$  with a half-life of 429 ms and  $^{98}\text{Sr}$  with a half-life of 653 ms could be used for nuclear spectroscopy experiments (the heaviest stable isotope of Sr is  $^{88}\text{Sr}$ ).

Although the  $Q_\beta$ -value of a neutron-rich  $^{147}\text{La}$  is 5.4 MeV, the energy levels of its daughter  $^{147}\text{Ce}$  have been reported for only those below 0.92 MeV. With a total absorption clover detector, Y. Shima *et al.* (PRS-2) could identify over twenty excited levels of  $^{147}\text{Ce}$  in the energy range from 1.0 to 2.7 MeV. The sum spectrum taken with the detector exhibits peaks, each of which directly corresponds to the energy of an excited level of  $^{147}\text{Ce}$ , its parents being available in KUR-ISOL.

The half-life of the nucleus is one of clues to understanding the nuclear structure. Using a radiation detection system consisting of one thin plastic and one  $\text{LaBr}_3$  scintillators, a feasibility test of which was done in the previous period, Y. Kojima *et al.* (PRS-3) measured the lifetime of the 98.2-keV level of  $^{148}\text{Pr}$ , its

parents being obtained in KUR-ISOL. From the value of 8.5(5) ns and the calculated internal conversion coefficient, they determined the reduced transition probability  $B(E2)$  to be 68(4) in Weisskopf units, indicating that the transition is of collective character.

Zinc oxide, a semiconductor with a relatively large band gap, has several favorable properties in materials science. W. Sato *et al.* (PRS-4a) measured at room temperature, using the TDPAC technique, the local electric field gradient at  $^{111}\text{Cd}$  ( $\leftarrow^{111\text{m}}\text{Cd}$ ) introduced in 0.5 at.% In- and 0.5 at.% Cd-doped ZnO. The pattern of the TDPAC spectrum is essentially the same as that for  $^{111}\text{Cd}$  ( $\leftarrow^{111}\text{In}$ ) in undoped ZnO, but very different from the case of  $^{111}\text{Cd}$  ( $\leftarrow^{111}\text{In}$ ) in 0.5 at.% In-doped ZnO, which means that depending on the parent element, the local structure around the same daughter nuclear probe can be different in this oxide.

S. Komatsuda *et al.* (PRS-4b) took a room-temperature TDPAC spectrum of  $^{111}\text{Cd}$  ( $\leftarrow^{111\text{m}}\text{Cd}$ ) introduced in 10 at.% Al-doped ZnO and compared it with that of  $^{111}\text{Cd}$  ( $\leftarrow^{111}\text{In}$ ) in  $10^{-5}$  at.% (= 0.1 ppm) Al-doped ZnO. It is shown that Al-In interactions are much stronger than Al-Cd interactions in ZnO.

S. Kitao *et al.* (PRS-5) measured the  $^{57}\text{Fe}$ -Mössbauer spectra for a non-superconductor  $\text{LaFeAsO}$  and a superconductor  $\text{LaFeAsO}_{1-x}\text{F}_x$  under the external magnetic field in order to obtain information on the nature of magnetism in these compounds. They concluded that Fe in both singlet phases assumed no magnetic moment (small if any) and that the magnetically ordered phase of  $\text{LaFeAsO}$  was antiferromagnetic.

Using the TDPAC technique, E. Imagawa *et al.* (PRS-6) measured at a temperature a little below room temperature the electric field gradient (EFG) at  $^{111}\text{Cd}$  ( $\leftarrow^{111}\text{Ag}$ ) incorporated in mavicyanin, a protein having a single metal site, with the help of a newly adopted chemical procedure. The present aim of the experiment is to compare the results with those previously obtained for  $^{111}\text{Cd}$  ( $\leftarrow^{111}\text{In}$ ) adsorbed in mavicyanin. As in the latter sample, dynamic behavior of the protein was observed in the former sample, giving a similar value of correlation time, but a very different EFG value.

Silver iodide is an ionic conductor, its high-temperature  $\alpha$ -phase exhibiting superionic conductivity but its low-temperature  $\beta$ - and  $\gamma$ -phases being of low conductivity. When the particle size becomes small to about 10 nm, the  $\alpha$ -phase survives down to 30°C. 11-nm  $\beta$ -/ $\gamma$ -AgI nanoparticles show the highest conductivity for a binary solid at room temperature. R. Makiura *et al.* (PRS-7) synthesized 10-nm AgI nanoparticles and took the synchrotron X-ray powder diffraction profiles in order to study the relationship between structural changes and ionic conduction before doing  $^{129}\text{I}$ -Mössbauer experiments on this system.

A.Taniguchi, Y. Ohkubo, M.Tanigaki, H. Hayashi<sup>1#</sup>, M. Shibata<sup>1</sup> and Y. Kojima<sup>2\*</sup>

Research Reactor Institute, Kyoto University

<sup>1</sup>Radioisotope Research Center, Nagoya University

<sup>2</sup>Graduate School of Engineering, Hiroshima University

**INTRODUCTION:** RI (Radioactive Ion) beam facilities are required to supply unstable nuclides of as many kinds and high intensities as possible for the studies of the nuclear structure and the application. At KUR-ISOL (KyoUki University Reactor-Isotope Separator On-Line), unstable nuclear beams mainly of alkali, alkaline-earth and rare earth nuclides produced from the thermal fission of <sup>235</sup>U have been developed. As for Sr and Ba isotopes, the fluorination method had been investigated in order to realize their efficient ionization [1]. However, this method have never been used especially for Sr isotopes heavier than <sup>97</sup>Sr because of their short half-lives for a gas-jet type of ISOL and the yields were expected not to be high although the fission yields are relatively high. On the other hand, with respect to the nuclear structure, nuclei in the Z~40 and N~60 region are interesting because the shape coexistence was found in the region [2]. Therefore, in this work, heavier Sr nuclides were focused, and their availability was researched at KUR-ISOL.

**EXPERIMENTS:** The <sup>235</sup>UF<sub>4</sub> of 50 mg was irradiated at a through tube facility of KUR. The fission products were transported using the He/N<sub>2</sub> gas-jet system to a surface-ionization type ion-source. The ionized activities were mass-separated using an electromagnet and collected on an aluminized Mylar tape, and the yields were measured by detecting representative  $\gamma$ -rays with a Ge detector. The Ge detector, whose relative efficiency was about 30%, was placed at an in-beam position and the distance from the source to the detector was 3 cm. In this experiment, the value of the magnetic field was first set to see <sup>92</sup>, <sup>93</sup>, <sup>95</sup>Sr, familiar nuclei to us, and then changed for heavier Sr isotopes while monitoring  $\gamma$ -rays. The input power to the ion source and the flow rates of the carrier gases were also appropriately adjusted using the <sup>92</sup>, <sup>93</sup>, <sup>95</sup>Sr beams.

**RESULTS:** Figures 1(a) and 1(b) show the  $\gamma$ -ray energy spectra of the mass number A=97 and A=98, respectively. As seen in these spectra, representative  $\gamma$ -rays of <sup>97</sup>Sr ( $T_{1/2}$ = 429 ms) and <sup>98</sup>Sr ( $T_{1/2}$ = 653 ms) were observed clearly. In particular, <sup>97</sup>Sr is a nuclide having the shortest half-life of 429 ms among the isotopes available at KUR-ISOL. Incidentally, the previous nuclide with the shortest half-life was <sup>150</sup>La ( $T_{1/2}$ = 510 ms) [3].

**CONCLUSION:** Focusing on the heavier Sr isotopes at

KUR-ISOL,  $\gamma$ -rays emitted from <sup>97</sup>, <sup>98</sup>Sr were observed, and it has been confirmed that these isotopes would be available for nuclear spectroscopy experiments. Moreover, the capability of using shorter half-life isotopes was shown from the viewpoint of performance of an ISOL coupled to a gas-jet system. Concerning Sr isotopes, it might be demonstrated in more careful and longer measurements that still heavier and shorter half-life Sr isotopes would be available.

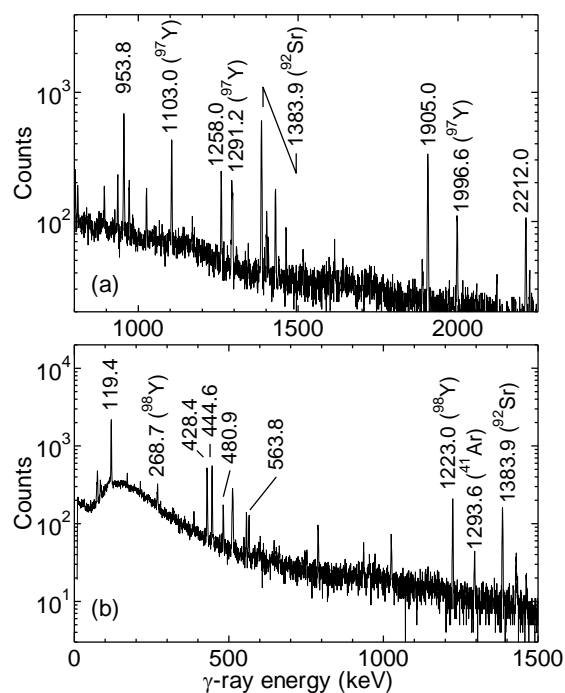


Fig. 1. The  $\gamma$ -ray spectra of (a) A=97(a) and (b) A=98. Representative  $\gamma$ -rays of <sup>97</sup>Sr, <sup>98</sup>Sr and their daughter nuclides were observed. The accumulation times of these spectra were 20 min and 6 min, respectively. The  $\gamma$ -ray peak of <sup>92</sup>Sr appeared in both spectra came from <sup>92</sup>Sr which were scattered to the inner wall of the tape chamber when they were extracted to the in-beam position and remained as a background component.

#### REFERENCES:

- [1] Y. Kawase *et al.*, Nucl. Instr. Meth. B **70** (1992) 146-149.
- [2] J. A. Pinston *et al.*, Phys. Rev. C **71** (2005) 064327.
- [3] K. Okano *et al.*, Z. Phys. A **351** (1993) 243-244.

# Present address. School of Health Sciences, The University of Tokushima Graduate School.

\* Present address. Radioisotope Research Center, Nagoya University.

## PR2-2 Decay Spectroscopy of $^{147}\text{La}$ with a Total Absorption Clover Detector

Y. Shima, H. Hayashi<sup>1#</sup>, M. Shibata<sup>1</sup>, Y. Kojima<sup>2\*</sup> and A. Taniguchi<sup>3</sup>

Graduate School of Engineering, Nagoya University

<sup>1</sup>Radioisotope Research Center, Nagoya University

<sup>2</sup>Graduate School of Engineering, Hiroshima University

<sup>3</sup>Research Reactor Institute, Kyoto University

**INTRODUCTION:** A total absorption clover detector has been developed [1] to measure  $\beta$ -decay energies ( $Q_{\beta}$ -value) of low-yield nuclides far from stability. In the measurement,  $\beta$ -rays and subsequent  $\gamma$ -rays are absorbed with high efficiency by the detector, and the  $Q_{\beta}$  is obtained from the endpoint of the spectrum. In addition, cascade  $\gamma$ -rays are also absorbed with high efficiency, and sum peaks corresponding to the energy of excited levels are observed in the spectrum. Thus, nuclear levels can be determined with this detector.

The  $Q_{\beta}$ -value of  $^{147}\text{La}$  was reported to be 5366 keV [2], but levels of  $^{147}\text{Ce}$  have been reported only up to 924.3 keV [3]. Therefore, it is expected that  $^{147}\text{Ce}$  has much higher levels. To identify high energy levels of  $^{147}\text{Ce}$ ,  $\gamma$ -rays following the decay of  $^{147}\text{La}$  were measured with the total absorption clover detector in this work.

### TOTAL ABSORPTION CLOVER DETECTOR:

The total absorption clover detector is composed of four Ge crystals, each 80 mm in diameter and 90 mm in length. These Ge crystals are arranged as if to form a four-leaf clover. Then, there is one through hole, 15 mm in diameter, along the central axis of the detector. Radioactive sources can be put into the through hole with a solid angle of almost  $4\pi$ , so that  $\gamma$ -rays are measured with high detection efficiency.

**EXPERIMENTS:** Neutron-rich  $^{147}\text{La}$  was produced with neutron-induced fission of  $^{235}\text{U}$ . The 93% enriched  $\text{UF}_4$  of 50 mg was irradiated by a thermal neutron flux of  $3 \times 10^{12}$  n/cm<sup>2</sup>/s.  $^{147}\text{La}$  was separated by the Isotope Separator On-line (ISOL). The mass-separated isotopes were collected on an aluminized Mylar tape. Then the source was moved to the center of the detector and subjected to a measurement. The collecting and measurement time was adjusted to two times the half-life of  $^{147}\text{La}$ , respectively. A pair of semicircular plastic sticks was put into the through hole of the detector to stop  $\beta$ -rays.

**ANALYSIS AND RESULTS:** Energy signals of each Ge crystal were independently amplified, and these energy signals together with the corresponding time information were stored using a data acquisition system in the event-by-event mode. The “Singles  $\times 4$ ” spectrum, namely, the sum of the four singles spectra taken with the Ge crystals, and the “Sum” spectrum, namely, the energy

sum spectrum, were obtained using an off-line sorting program.

Figure 1 shows a part of the measured spectra of  $^{147}\text{La}$  using the total absorption clover detector. Many  $\gamma$ -ray peaks are observed above 1.5 MeV. Sum peaks are strongly observed in the Sum spectrum compared to the Singles  $\times 4$  one. From the Sum spectrum, more than twenty levels from 1.0 MeV to 2.7 MeV in  $^{147}\text{Ce}$  were identified. Then, cascade relations were confirmed by  $\gamma$ - $\gamma$  coincidence spectra. The closed circle indicates newly identified levels in  $^{147}\text{Ce}$ .

**CONCLUSIONS:** Neutron-rich  $^{147}\text{La}$  was studied using a total absorption clover detector, and more than twenty levels in  $^{147}\text{Ce}$  were identified for the first time. Determination of the intensities of the newly observed  $\gamma$ -rays is now in progress.

**ACKNOWLEDGEMENTS:** This study is partially supported by “Study on nuclear data by using a high intensity pulsed neutron source for advanced nuclear system” entrusted to Hokkaido University by the Ministry of Education, Culture, Sports, Science and Technology of Japan (MEXT).

### REFERENCES:

- [1] M. Shibata *et al.*, JAEA-Tokai Tandem Annual Report 2010, JAEA-Review **2010-056** (2010) 19.
- [2] H. Hayashi *et al.*, Nucl. Instrum. Meth. A **606** (2009) 484.
- [3] J. D. Robertson *et al.*, Phys. Rev. **40** (1989) 2804.

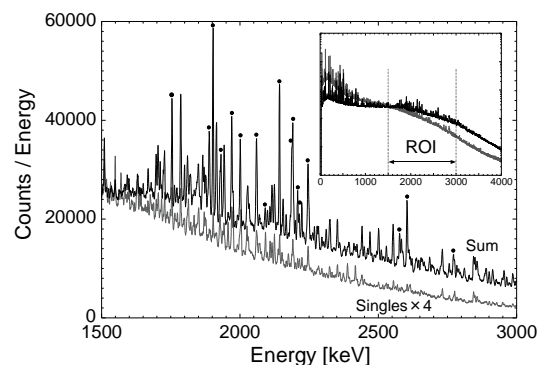


Fig.1. A part of the Singles  $\times 4$  spectrum and the Sum spectrum around 2.0 MeV measured with the total absorption clover detector. The closed circles indicate sum peaks corresponding to newly observed levels in  $^{147}\text{Ce}$ . The inset shows the overview of the spectra.

# Present address. School of Health Science, The University of Tokushima Graduate School.

\* Present address. Radioisotope Research Center, Nagoya University.

採択課題番号 22P2-2 オンライン同位体分離装置を用いた質量数 150 近傍の  
核分裂生成物の崩壊核分光 プロジェクト

(名大・RIC) 柴田理尋、林 裕晃 (名大院・工) 嶋 洋佑 (広大院・工) 小島康明  
(京大・原子炉) 谷口秋洋 (名大・工) 高木 孝

Y. Kojima\*, H. Hayashi<sup>1#</sup>, M. Shibata<sup>1</sup>, S. Higuma,  
T. Fukushige, K. Shizuma and A. Taniguchi<sup>2</sup>

Graduate School of Engineering, Hiroshima University

<sup>1</sup>Radioisotope Research Center, Nagoya University

<sup>2</sup>Research Reactor Institute, Kyoto University

**INTRODUCTION:** Many spectroscopic studies have been performed on fission products around mass number of 150 because they provide an opportunity to study transition from the spherical to the deformed nuclei. For example, Hayashi et al. reported that the experimental  $\beta$  decay energies for  $^{147-149}\text{La}$  deviated from the theoretically evaluated values [1]. This strongly suggests that an unexpected nuclear structure change exists.

To investigate nuclear structure around  $^{147-149}\text{La}$  through level lifetime measurements, we developed a new spectrometer consisting of a thin plastic and a  $\text{LaBr}_3$  scintillator in FY2009 [2]. Excellent time resolutions observed for our spectrometer (380 ps for 1332 keV  $\gamma$  ray) will enable lifetime determination down to sub-nanosecond. In 2010, we installed this spectrometer to the on-line isotope separator KUR-ISOL, and applied lifetime measurements for mass-separated  $^{148}\text{Pr}$ , of which lifetimes had not been reported for any excited levels.

**EXPERIMENTS:** The on-line experiments were performed separately for two stages. First, the well-evaluated level lifetimes in  $^{93}\text{Sr}$  and  $^{148}\text{Ce}$  were measured to demonstrate that our spectrometer deduces lifetimes without any systematic error. Next, a level lifetime of  $^{148}\text{Pr}$  was newly measured.

The parent nuclides  $^{93}\text{Rb}$ ,  $^{148}\text{La}$  and  $^{148}\text{Ce}$  were prepared at KUR-ISOL, following the thermal-neutron induced fission of  $^{235}\text{U}$ . The mass-separated ions were implanted into an aluminized Mylar tape in a computer-controlled tape transport system. The radioactive sources were periodically moved to a measuring port where the spectrometer described above was set up. At the detector station, a high-resolution Ge detector was also placed to check contaminations and to select a desired decay branch through an off-line sorting. The  $\beta$ - $\gamma$ - $\gamma$  triple coincidence data were recorded in a list mode.

**RESULTS and DISCUSSION:** Figure 1(a) shows the decay curve of the 158.5 keV level in  $^{148}\text{Ce}$ . It was obtained through gating on the 158.5 keV  $\gamma$  ray detected by the  $\text{LaBr}_3$  detector. From the clearly observed slope, the lifetime of 1.49(7) ns was obtained via the least-square fitting using an exponential function. Our results agree well with the evaluated lifetime of 1.46(9) ns [3].

The decay curve obtained through gating on a  $\gamma$  energy region of 205-230 keV in a mass fraction of 93 also showed a long tail. This  $\gamma$  peak is a doublet of the 213.4 and 219.2 keV  $\gamma$  rays from excited levels in  $^{93}\text{Sr}$ . Here, the 219 keV  $\gamma$  ray is a transition from the very short-lived

433 keV level (lifetime < 0.4 ns [3]). Hence, the long slope is due to the decay of the 213 keV level in  $^{93}\text{Sr}$ . The lifetime of 6.48(10) ns obtained from the slope is in good agreement with the previous value of 6.6(4) ns [3]. These two results on  $^{148}\text{Ce}$  and  $^{93}\text{Sr}$  show that our spectrometer is sufficiently capable of measuring level lifetimes of mass-separated fission products.

For the  $\beta$  decay of  $^{148}\text{Ce}$ , a delay component was observed in the time spectrum gated on the 99 keV  $\gamma$  peak measured with the  $\text{LaBr}_3$  detector. This 99 keV peak is a triplet of the 98.0, 98.2 and 99.0 keV  $\gamma$  rays. To select the  $\gamma$  branch unambiguously, additional gates were set on the  $\gamma$  rays detected by the Ge detector. Among them, the time spectrum coincident with the 98.0 keV (Fig. 1(b)) and that with 191.6 keV showed long slopes. This means the delay component is due to the 98.2 keV level in  $^{148}\text{Pr}$ . The averaged value of 8.5(5) ns was adopted for the lifetime of the 98.2 keV level. It was newly obtained in this work. Using the experimental lifetime and the total internal conversion coefficient of 2.26, the reduced transition probability  $B(E2)$  was evaluated to be 68(4) in the Weisskopf unit. This value roughly agrees with typical  $B(E2)$  of  $\sim 10^2$  for collective  $E2$  transitions. Further discussion will be given after more detailed  $\gamma$  spectroscopy.

**CONCLUSIONS:** A new spectrometer installed to KUR-ISOL was successfully applied for lifetime measurements in a time range around nanosecond. The lifetime of 8.5(5) ns was obtained for the 98.2 keV level in  $^{148}\text{Pr}$  for the first time.

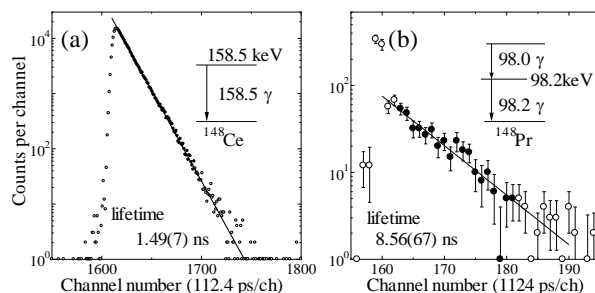


Fig. 1. (a) Decay curves of the 158.5 keV level in  $^{148}\text{Ce}$  and (b) that of the 98.2 keV level in  $^{148}\text{Pr}$ .

#### REFERENCES:

- [1] H. Hayashi *et al.*, Nucl. Instr. Meth. A, **606** (2009) 484-489.
- [2] Y. Kojima and K. Shizuma, KURRI Prog. Rep. **2009** (2010) 124.
- [3] Evaluated Nuclear Structure Data File (ENSDF), <http://www.nndc.bnl.gov/ensdf>.

\* Present address. Radioisotope Research Center, Nagoya University.

# Present address. School of Health Sciences, The University of Tokushima Graduate School.

W. Sato, S. Komatsuda<sup>1</sup> and Y. Ohkubo<sup>2</sup>

*Institute of Science and Engineering, Kanazawa University*

<sup>1</sup>*Graduate School of Science and Technology, Kanazawa University*

<sup>2</sup>*Research Reactor Institute, Kyoto University*

**INTRODUCTION:** Zinc oxide (ZnO) is an intrinsic *n*-type semiconductor having optoelectronic properties. For its wider industrial application as semiconductor devices, it is important to study the *n*-type conductivity realized by impurity doping on an atomic scale. In our previous work, we investigated the local field at the In donor site in In-doped ZnO by means of the time-differential perturbed angular correlation (TDPAC) method with the <sup>111</sup>Cd probe formed in the disintegration of <sup>111</sup>In [1]. We successfully obtained intriguing TDPAC spectra exhibiting a high frequency component, which is distinct from the one appearing in the corresponding spectrum for undoped ZnO; however, the origin of the component is still unknown. In order to identify the component, we examined the local structure at the same probe <sup>111</sup>Cd but disintegrated from different parent <sup>111m</sup>Cd introduced in In-doped ZnO. Based on a well-defined TDPAC spectrum, in the present report, we discuss different interacting natures of the two probes, <sup>111</sup>Cd( $\leftarrow$ <sup>111</sup>In) and <sup>111</sup>Cd( $\leftarrow$ <sup>111m</sup>Cd), with 0.5 at.% doped In.

**EXPERIMENTS:** About 3 mg of cadmium oxide (CdO) enriched with <sup>110</sup>Cd was irradiated with thermal neutrons in a pneumatic tube at Kyoto University Reactor, and radioactive <sup>111m</sup>Cd was prepared. The neutron-irradiated CdO powder was then added into stoichiometric amount of 0.5 at.% In-doped ZnO powder to synthesize 0.5 at.% In- and 0.5 at.% Cd-codoped ZnO. (It is to be noted that the 0.5 at.% nonradioactive Cd is inevitably incorporated in the sample.) The powder was thoroughly mixed until uniformity was achieved. The mixture was then pressed into a disk, and sintered in air at 1373 K for 45 min. TDPAC measurements were performed for the sintered sample at room temperature for the probe <sup>111</sup>Cd( $\leftarrow$ <sup>111m</sup>Cd) on the 151-245 keV cascade  $\gamma$  rays with the intermediate state of  $I = 5/2$  having a half-life of 85 ns.

**RESULTS:** In Fig. 1(a) is shown the TDPAC spectrum of <sup>111m</sup>Cd embedded in 0.5 at.% In- and 0.5 at.% Cd-codoped ZnO (denominated <sup>111m</sup>Cd-ICZO), and in Fig. 1(b) the one of <sup>111</sup>In in 0.5 at.% In-doped ZnO (<sup>111</sup>In-IZO), cited from Ref. [1] for comparison. The measurements were performed at room temperature for both samples. The directional anisotropy on the ordinate,  $A_{22}G_{22}(t)$ , was deduced with the following simple operation:

$$A_{22}G_{22}(t) = \frac{2[N(\pi, t) - N(\pi/2, t)]}{N(\pi, t) + 2N(\pi/2, t)}. \quad (1)$$

Here,  $A_{22}$  denotes the angular correlation coefficient,  $G_{22}(t)$  the time-differential perturbation factor as a function of the time interval,  $t$ , between the relevant cascade  $\gamma$ -ray emissions, and  $N(\theta, t)$  the number of the delayed coincidence events observed at an angle,  $\theta$ . The oscillating frequencies in the spectra are obviously different, but both of the spectral patterns reflect typical electrostatic interactions between the probe nucleus and the surrounding charge distribution for  $I = 5/2$ . A least-squares fits were thus performed with basically the same  $G_{22}(t)$  function written as

$$G_{22}(t) = G_{22}^*(t) \left[ \sigma_{2,0} + \sum_{n=1}^3 \sigma_{2,n} \cos(\omega_n t) \right]. \quad (2)$$

For all the symbols in Eq. (2), refer to our previous paper [1]. The magnitude of the electric field gradient at the probe nucleus in <sup>111m</sup>Cd-ICZO was deduced from the fit to be  $1.8(3) \times 10^{21} \text{ Vm}^{-2}$ , which agrees well with that for undoped ZnO [1]. It is evident from this observation that the probe in <sup>111m</sup>Cd-ICZO solely resides at the substitutional Zn site feeling little perturbation from the nonradioactive In impurities. As regards the spectrum for <sup>111</sup>In-IZO in Fig. 1(b), a distinct perturbation pattern with a single higher-frequency component appears in spite of the same <sup>111</sup>Cd probe [1]. These observations lead to the following consequence: it is the <sup>111</sup>Cd probe as the EC decay product of <sup>111</sup>In but not as the IT product of <sup>111m</sup>Cd that has a unique interaction with the nonradioactive In ion(s). Detailed discussion on the local structure is now underway from the viewpoint of Coulomb interaction between In ions.

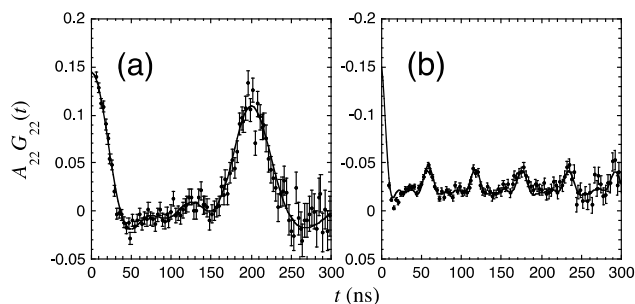


Fig. 1. Room-temperature TDPAC spectra (a) of <sup>111m</sup>Cd( $\leftarrow$ <sup>111m</sup>Cd) in <sup>111m</sup>Cd-ICZO and (b) of <sup>111</sup>Cd( $\leftarrow$ <sup>111</sup>In) in <sup>111</sup>In-IZO. For the abbreviations for the names of the samples, see the text.

#### REFERENCE:

[1] W. Sato *et al.*, *Phys. Rev. B* **78** (2008) 045319 (1-5).

## PR2-5 Observation of a Local Field at the $^{111}\text{Cd}(\leftarrow^{111\text{m}}\text{Cd})$ Probe in Al-Doped ZnO

S. Komatsuda, W. Sato<sup>1</sup> and Y. Ohkubo<sup>2</sup>

Graduate School of Natural Science and Technology,  
Kanazawa University

<sup>1</sup>Institute of Science and Engineering, Kanazawa University

<sup>2</sup>Research Reactor Institute, Kyoto University

**INTRODUCTION:** Zinc oxide (ZnO) doped with group 13 elements (Al, Ga, In) as impurity donors is expected for application to functional devices as *n*-type semiconductors. For a practical use of ZnO as a conduction-controlling device, it is of great importance to study the physical and chemical states of dilute impurity ions in ZnO. In the present work, we have found from the result of a time-differential perturbed angular correlation (TDPAC) study applied to Al-doped ZnO that the  $^{111}\text{Cd}(\leftarrow^{111}\text{In})$  probe is perturbed by the effect of Al doping even at the extremely dilute Al concentration of 0.1 ppm. This experimental result implies that there is a strong attractive force between Al ion(s) and the  $^{111}\text{Cd}(\leftarrow^{111}\text{In})$  probe. In order to investigate whether this attractive force is characteristic of the interaction between  $^{111}\text{In}$  and Al ions, we performed a TDPAC measurement for Al-doped ZnO with the same  $^{111}\text{Cd}$  probe but disintegrated from a different parent nucleus,  $^{111}\text{Cd}(\leftarrow^{111\text{m}}\text{Cd})$ . Based on the spectral pattern, we discuss the local structure in the vicinity of the probes in Al-doped ZnO [1].

**EXPERIMENTS:** For the synthesis of 10 at.% Al-doped ZnO, stoichiometric amounts of  $\text{Al}(\text{NO}_3)_3 \cdot 9\text{H}_2\text{O}$  and ZnO powder were mixed in ethanol. The suspension was heated to evaporate the ethanol until dryness. The powder was pressed into a disk and sintered in air at 1273 K for 3 h. As for the synthesis of the  $^{111}\text{Cd}(\leftarrow^{111\text{m}}\text{Cd})$  probe, about 3 mg of cadmium oxide enriched with  $^{110}\text{Cd}$  was irradiated with thermal neutrons in a pneumatic tube at Kyoto University Reactor. In order to prepare a sample for a TDPAC measurement, we mixed the radioactive cadmium oxide with the Al-doped ZnO synthesized above, pressed the mixture into a disk, and sintered it in air at 1373 K for 45 min. The TDPAC measurement was carried out for the 151-245 keV cascade  $\gamma$  rays of  $^{111}\text{Cd}(\leftarrow^{111\text{m}}\text{Cd})$  probe with the intermediate state of  $I = 5/2$  having a half-life of 85.0 ns.

**RESULTS:** Figure 1(a) shows the TDPAC spectrum of  $^{111}\text{Cd}(\leftarrow^{111\text{m}}\text{Cd})$  embedded in 10 at.% Al-doped ZnO. For comparison, the spectrum for 0.1 ppm Al-doped ZnO is cited from Ref. [1] in Fig. 1(b). The directional anisotropy on the ordinate,  $A_{22}G_{22}(t)$ , was deduced with the following simple operation for delayed coincidence events of the cascade:

$$A_{22}G_{22}(t) = \frac{2[N(\pi, t) - N(\pi/2, t)]}{N(\pi, t) + 2N(\pi/2, t)}$$

Here,  $A_{22}$  denotes the angular correlation coefficient,  $G_{22}(t)$  the time-differential perturbation factor as a function of the time interval,  $t$ , between the relevant cascade  $\gamma$ -ray emissions, and  $N(\theta, t)$  the number of the coincidence events observed at an angle,  $\theta$ . The oscillating pattern in Fig. 1(a) reflects typical electrostatic interaction between the probe nucleus and the surrounding charge distribution for  $I = 5/2$ , and shows a similar pattern to that for undoped ZnO [2]. This observation suggests that the probe ions reside solely at the substitutional Zn site being independent of the field produced by the Al ions. While the  $^{111}\text{Cd}(\leftarrow^{111}\text{In})$  probe can be associated with Al ion(s) even at the extremely dilute Al concentration of 0.1 ppm, the  $^{111}\text{Cd}(\leftarrow^{111\text{m}}\text{Cd})$  probe is not affected by the field produced by the Al doping in spite of the presence of a large amount of Al ions in the system. This observation clearly suggests that it is the  $^{111}\text{Cd}$  probe disintegrated from  $^{111}\text{In}$  but not from  $^{111\text{m}}\text{Cd}$  that feels a strong perturbation by Al ion(s). We found from this observation that there is a strong attractive force characteristic of In and Al in ZnO. For further information, it is necessary to investigate how the In ions are associated with Al in ZnO.

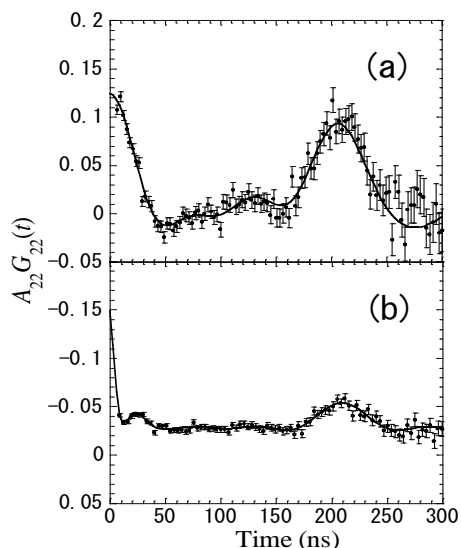


Fig. 1. Room-temperature TDPAC spectra (a) of  $^{111}\text{Cd}(\leftarrow^{111\text{m}}\text{Cd})$  in 10 at.% Al-doped ZnO and (b) of  $^{111}\text{Cd}(\leftarrow^{111}\text{In})$  in 0.1 ppm Al-doped ZnO.

### REFERENCES:

- [1] S. Komatsuda *et al.*, submitted to *J. Phy. Soc. Jpn.*
- [2] W. Sato *et al.*, *Phys. Rev. B* **78** (2008) 045319 (1-5).

## PR2-6 Mössbauer Study of LaFeAsO and LaFeAsO<sub>1-x</sub>F<sub>x</sub> in External Magnetic Fields

S. Kitao<sup>1,2</sup>, Y. Kobayashi<sup>1,2</sup>, M. Kurokuzu<sup>1,2</sup>, M. Saito<sup>1,2</sup>,  
H. Fukuma<sup>1,2</sup>, T. Mitsui<sup>2,3</sup>, Y. Kamihara<sup>4</sup>, M. Hirano<sup>5,6</sup>,  
H. Hosono<sup>5,6</sup> and M. Seto<sup>1,2,3</sup>

<sup>1</sup>Research Reactor Institute, Kyoto University

<sup>2</sup>CREST, Japan Science and Technology Agency

<sup>3</sup>Japan Atomic Energy Agency

<sup>4</sup>Keio University

<sup>5</sup>Tokyo Institute of Technology

<sup>6</sup>ERATO-SORST, Japan Science and Technology Agency

**INTRODUCTION:** The discoveries of Fe-oxipnictide superconductors, LaFePO [1] and LaFeAsO<sub>1-x</sub>F<sub>x</sub> [2], have just opened a new epoch of superconductivity. Since the discoveries, extensive researches have been performed to elucidate the mechanism of their superconductivity. Since the Fe is believed to act as a key element of the superconductivity, Fe-Mössbauer spectroscopy is one of the most essential methods to investigate the nature of the superconductivity. We have carried out Mössbauer studies on some Fe oxipnictides and revealed many important facts, e.g., the F-doping to the LaFeAsO suppresses the magnetic transition and leads to the emergence of superconductivity in LaFeAsO<sub>1-x</sub>F<sub>x</sub> [3]. In this study, we applied magnetic fields to derive more information from Mössbauer spectroscopy, since the nature of the magnetism can be more clearly elucidated by use of a magnetic field [4].

**EXPERIMENTS:** The Mössbauer experiments were carried out using a superconducting magnet at the magnetic field up to 14 T. The magnetic field was applied parallel to the gamma-ray direction. A <sup>57</sup>Co source in Rh matrix with a nominal activity of 1.85 GBq was positioned inside a cancellation magnet. The isomer shifts of the velocity scale are referenced to  $\alpha$ -Fe. The LaFeAsO<sub>1-x</sub>F<sub>x</sub> and LaFeAsO samples were synthesized by the method described elsewhere [2]. The electric resistivity measurement of the F-doped sample showed a transition temperature of 24 K for  $x=0.07$ . The LaFeAsO did not undergo a superconducting transition, but had a magnetic transition at Néel temperature ( $T_N$ ) of  $\sim 140$  K.

**RESULTS AND DISCUSSION:** The F-doped superconductor LaFeAsO<sub>1-x</sub>F<sub>x</sub> and high-temperature phase of the parent LaFeAsO above  $T_N$ , both of which showed singlet spectra, were studied with external magnetic fields. Typical Mössbauer spectra under the external magnetic field up to 14 T for the LaFeAsO<sub>0.93</sub>F<sub>0.07</sub> at 2 K and for LaFeAsO at 200 K are shown in Fig. 1. The observed magnetic fields were comparable to the external magnetic fields and any additional magnetic order was not apparently induced by the external magnetic field. This observation supports that the Fe in the singlet phase does not have any magnetic moment, or that it should be small if any. On the other hand, the parent LaFeAsO showed magnetically-split spectra at low temperatures. The Mössbauer spectra observed under the magnetic field, as seen in Fig. 2 show intermediate states of the magnetic

moments aligned to the direction of the external field. The spectra were well described by an analytic model of polycrystalline antiferromagnets under the external magnetic field, which uses an atomic spin Hamiltonian [5]. The fact that the model successfully describes the observed spectra clearly proves the magnetically ordered phase is antiferromagnetic.

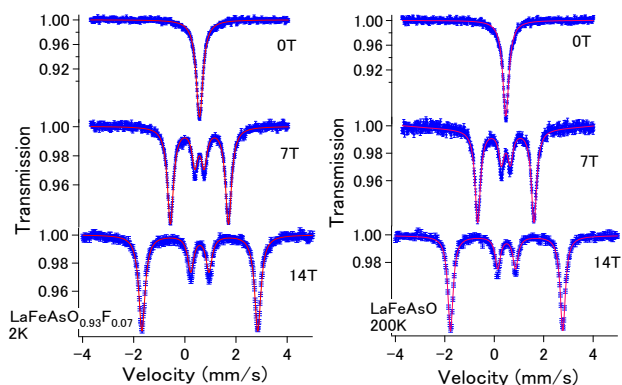


Fig. 1. Mössbauer spectra under magnetic fields of LaFeAsO<sub>0.93</sub>F<sub>0.07</sub> at 2 K and LaFeAsO at 200 K.

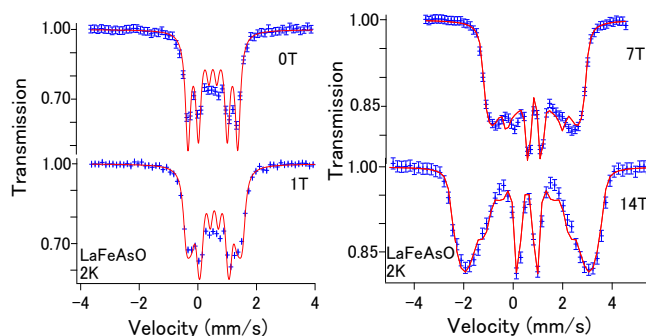


Fig. 2. Mössbauer spectra under magnetic fields of LaFeAsO at 2 K.

### REFERENCES:

- [1] Y. Kamihara, H. Hiramatsu, M. Hirano, R. Kawamura, H. Yanagi, T. Kamiya and H. Hosono, *J. Am. Chem. Soc.* **128** (2006)10012.
- [2] Y. Kamihara, T. Watanabe, M. Hirano and H. Hosono, *J. Am. Chem. Soc.* **130** (2008) 3296.
- [3] S. Kitao, Y. Kobayashi, S. Higashitaniguchi, M. Saito, Y. Kamihara, M. Hirano, T. Mitsui, H. Hosono and M. Seto, *J. Phys. Soc. Jpn.* **77** (2008) 103706.
- [4] S. Kitao, Y. Kobayashi, S. Higashitaniguchi, M. Kurokuzu, M. Saito, T. Mitsui, Y. Kamihara, M. Hirano, H. Hosono and M. Seto, *J. Phys.: Conf. Ser.* **217** (2010) 012120.
- [5] Q. A. Pankhurst and R. J. Pollard, *J. Phys.: Condens. Matter* **2** (1990) 7329.



## Dynamics of Mavicyanin Observed by the PAC Method Using the $^{111}\text{Cd}$ ( $\leftarrow^{111}\text{Ag}$ ) Probe

E. Imagawa, A. Yokoyama<sup>1</sup>, W. Sato<sup>1</sup>, K. Kataoka<sup>1</sup>  
and Y. Ohkubo<sup>2</sup>

*Faculty of Science, Kanazawa University*

<sup>1</sup>*Faculty of Chemistry, Institute of Science and Engineering, Kanazawa University*

<sup>2</sup>*Research Reactor Institute, Kyoto University*

**INTRODUCTION:** The structure around the metal site of mavicyanin, a protein molecule with a single copper site, was investigated by using time-differential perturbed angular correlation (TDPAC) of  $\gamma$ -rays from the probe nuclei  $^{111}\text{Cd}(\leftarrow^{111}\text{Ag})$  and  $^{111}\text{Cd}(\leftarrow^{111}\text{In})$  [1,2]. In the previous study for the protein by using the  $^{111}\text{Ag}$  parent nuclei [1], we assumed that there might be several possible sites where the probe nuclei are adsorbed, so that we were not able to resolve each component due to insufficient counting statistics.

In the present study,  $^{111}\text{Ag}$  parent nuclei ( $T_{1/2} = 7.45\text{d}$ ) were introduced into mavicyanin and they were settled well in a unique site in the protein with the aid of a newly adopted procedure including dialysis for the sample preparation. We here report successful observation of dynamic behavior of mavicyanin in the solution showing its specific time scale.

**EXPERIMENTS:** The parent nuclei  $^{111}\text{Ag}$  were obtained by irradiating metal foil of Pd of natural abundance with thermal neutrons at KURRI. The nuclei were produced via the  $^{110}\text{Pd}(n, \gamma)^{111}\text{Pd}$  reaction followed by  $\beta$  decay of  $^{111}\text{Pd}$  ( $T_{1/2} = 23.4\text{ min}$ ). The foil was dissolved in aqua regia and  $^{111}\text{Ag}$  was extracted through purification with an anion exchange process to prepare the tracer solution. The solution was mixed with another solution of  $60\mu\text{M}$  wild-type apo-mavicyanin, refolded from inclusion bodies and adjusted to pH 7.5 with Tris buffer, and the mixture was stirred constantly for 12 hours. In this

process, Ag ions were incorporated in the metal sites of mavicyanin. Then the solution was subjected to a dialysis process to eliminate unbound Ag ions. Finally, the sample solution obtained in the procedure above was analyzed by the PAC technique at a temperature of some degrees below room temperature while being cooled on a Peltier device.

**RESULTS:** The measured TDPAC spectrum for the sample solution leads one to assume two components contributing to it as reported previously in [2]. In the case, the adopted expression of  $G_{22}(t)$  as a function of the time interval between the cascade  $\gamma$ -ray emissions is given as:

$$G_{22}(t) = f \exp(-t/\tau_c) \left\{ \sigma_{2,0} + \sum_{n=1}^3 \sigma_{2,n} \cos(a_n \omega_Q t) \right\} + (1-f),$$

where  $f$  denotes the fraction of the component occupying the site of the protein,  $\tau_c$  the correlation time between the probe nucleus and the extranuclear field, and  $\omega_Q$  the electric quadrupole frequency.

Table 1 lists the parameter values obtained by a least squares fit for the measured spectrum with our previous result [2] for comparison. The fair agreement of the correlation time obtained in both experiments evidently signifies that the protein indeed shows dynamic motion in the present solution in the time scale of 20-30 ns. On the other hand, the different  $\omega_Q$  values show the occupation of the probes in different sites, suggesting different chemical behaviors of parent elements.

It is also demonstrated by a high value of  $f$  obtained in this study that the observed spectrum became clearer than that of our previous data [1] by employing the different desalting procedure with dialysis instead of column chromatography.

### REFERENCES:

- [1] I. Yamazaki *et al.*, KURRI Prog. Rep. **2007**, 115 (2008).  
[2] T. Kubota *et al.*, KURRI Prog. Rep. **2009**, 128 (2010).

Table 1. Parameter values obtained by least-squares fits.

Parent probe( $\rightarrow$ Daughter)	$\omega_Q$ (Mrad/s)	$f$	$\tau_c$ (ns)
$^{111}\text{Ag}(\rightarrow^{111}\text{Cd})$	31.2(11)	0.83(2)	24(7)
$^{111}\text{In}(\rightarrow^{111}\text{Cd})$ [2]	15.5(11)	0.58(2)	21(7)

R. Makiura, H. Kitagawa<sup>1</sup>, S. Kitao<sup>2</sup> and M. Seto<sup>2</sup>

Nanoscience and Nanotechnology Research Center,  
Osaka Prefecture University

<sup>1</sup>Graduate School of Science, Kyoto University

<sup>2</sup>Research Reactor Institute, Kyoto University

**INTRODUCTION:** Solid-state ionic conductors are actively studied for their large application potential in batteries and sensors. From the view of future nanodevices, nanoscaled ionic conductors are attracting much interest. Silver iodide (AgI) is a well-known ionic conductor whose high-temperature  $\alpha$ -phase shows a superionic conductivity greater than  $1 \Omega^{-1} \text{cm}^{-1}$ . Below  $147^\circ\text{C}$ ,  $\alpha$ -AgI undergoes a phase transition into the poorly conducting  $\beta$ - and  $\gamma$ -polymorphs, thereby limiting its applications. We have recently reported the facile synthesis of variable-size AgI nanoparticles coated with poly-*N*-vinyl-2-pyrrolidone (PVP) and the controllable tuning of the  $\alpha$ - to  $\beta$ -/ $\gamma$ -phase transition temperature ( $T_{c\downarrow}$ ) [1]. When the size approaches 10-11 nm, the  $\alpha$ -phase survives down to  $30^\circ\text{C}$  - the lowest temperature for any AgI family materials. Moreover, the conductivity of 11 nm  $\beta$ -/ $\gamma$ -AgI nanoparticles at  $24^\circ\text{C}$  is  $\sim 1.5 \times 10^{-2} \Omega^{-1} \text{cm}^{-1}$  - the highest ionic conductivity for a binary solid at room temperature. In order to study the origin of the high ionic conductivity, we planned to perform <sup>129</sup>I Mössbauer spectroscopy. We have also performed X-ray diffraction (XRD) measurements at low temperatures to investigate the relationship between structural changes and the ionic conduction.

**EXPERIMENTS:** Equimolar amounts of aqueous AgNO<sub>3</sub> (WAKO, 99.8%), and NaI (WAKO, 99.5%) solutions were mixed at room temperature in the dark in the presence of PVP (WAKO, K-30; average MW = 40,000). Resultant mixtures were membrane-filtered to remove water-soluble starting materials and NaNO<sub>3</sub>. The precipitate was dried in vacuum and a yellowish green film was obtained. Synchrotron X-ray powder diffraction data were collected following both heating and cooling protocols between  $-193$  and  $190^\circ\text{C}$  using a gas blower with the high-resolution powder diffractometer.

**RESULTS:** XRD profiles of 10 nm AgI nanoparticles are shown in Fig. 1. The dominant structure of the as-prepared AgI nanoparticles at  $21^\circ\text{C}$  is the  $\beta$ -polymorph. The  $\gamma$ -polymorph is also present. This phase assemblage

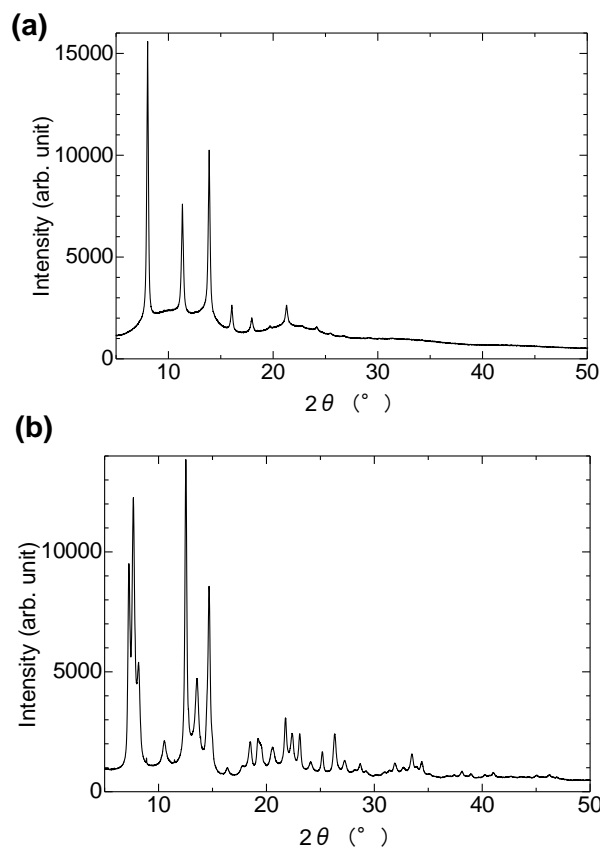


Fig. 1. XRD profiles of 10nm AgI nanoparticles (a) at  $183^\circ\text{C}$ , (b) at  $-197^\circ\text{C}$ .

remains stable on heating up to  $138^\circ\text{C}$ . Further heating leads to a gradual transformation to the  $\alpha$ -phase that is complete at  $165^\circ\text{C}$ . Between  $165$  and  $200^\circ\text{C}$ , only  $\alpha$ -AgI was observed (Fig. 1(a)). However, the  $\beta$ -/ $\gamma$ -  $\rightarrow$   $\alpha$ -phase transition is strongly thermally hysteretic and  $\alpha$ -phase is still observed at  $40^\circ\text{C}$ . The dominant structure at room temperature is  $\beta$ -phase and the  $\gamma$ -polymorph is also present. Below room temperature, the structural phase remains same up to  $-197^\circ\text{C}$  (Fig. 1(b)). We now try to confirm the synthetic condition so that AgI nanoparticles with <sup>129</sup>I can be fabricated for a <sup>129</sup>I Mössbauer study.

#### REFERENCE:

- [1] R Makiura, T. Yonemura, T. Yamada, M. Yamauchi, R. Ikeda, H. Kitagawa, and K. Kato, M. Takata, *Nature Mater.* **8** (2009) 476-480.